

Novel Codimension-two Bifurcation in a Coupled Duffing System with twisted frequency-response curves

Yung-Chia Hsiao^{1*} Ting-Yu Lai²

¹Assistant Professor of Department of Computer Science and
Information Engineering, MingDao University

²Graduate Student of Department of Mechanical Engineering,
National Central University

Abstract

This paper studied a novel codimension-two bifurcation combined by chaos and bifurcations of periodic orbits of period-1 and subharmonic orbits of period-2 in a coupled Duffing system with twisted frequency-response curves. A bifurcation line constructed by the saddle-node bifurcations of periodic orbits of period-1 tangentially intersects a bifurcation line constructed by the period doubling bifurcations of periodic orbits of period-1 at a codimension-two bifurcation point. Meanwhile, a Hopf bifurcation line constructed by the Hopf bifurcations of subharmonic orbits of period-2 merges into the codimension-two bifurcation point and then disappears. In this moment, chaos is generated simultaneously. To analyze the phenomenon, the periodic orbits and the subharmonic orbits are detected by using the shooting method and the frequency responses are obtained through the harmonic balance method. Besides, the stability of the obtained orbits is performed using the Floquet theory.

Keywords : bifurcation, codimension-two, chaos, Duffing System, subharmonic orbit

*通訊作者. Tel:04-8876660 ext.8116
Fax:04-8879050
E-mail: ycshaw@mdu.edu.tw

1. Introduction

Duffing equation is one of the common nonlinear differential equations with a harmonic driving force and cubic nonlinearity. Saddle-node bifurcations that a stable periodic orbit and an unstable periodic orbit are coalesced or generated each other are found in the Duffing equation. The famous “jump phenomenon” in the Duffing equation results from the saddle-node bifurcation point. The spring term of the Duffing equation is called “soft” if the signs of the linear spring term and cubic nonlinearity are opposite. When the sign of the coefficient of the linear spring is the same as the sign of the cubic nonlinearity, the spring term is called a hard spring. Normally, the nonlinearity bends the frequency-response curve of the system to the right for the hard springs. The jump phenomenon occurs at the right of the primary resonance. On the contrary, the frequency-response curve of the system is bended to the left and the jump phenomenon occurs in the left of the primary resonance for the soft springs. Sometimes, the frequency-response curve could be twisted in increasing the amplitude of the excitation. Szemplińska-Stupnicka portrayed that the frequency-response curve for the Duffing equation with hard spring is bended to the right in small amplitude of the frequency response, then to the left side in large amplitude of the frequency response, finally back to the right [Szemplińska-

Stupnicka, 1990].

This paper studied the nonlinear dynamics of the coupled Duffing equation with twisted frequency-response curves. A novel codimension-two bifurcation combined by chaos and bifurcations of periodic responses of period-1 and period-2 was observed in a large periodic excitation. With varying two parameters of the periodic excitation, a bifurcation line constructed by the saddle-node bifurcations of periodic orbits of period-1 tangentially intersects a bifurcation line constructed by the period doubling bifurcations of periodic orbits of period-1. Hsiao and Tung had studied the phenomenon [Hsiao & Tung, 2002]. Meanwhile, a Hopf bifurcation line constructed by Hopf bifurcations of the subharmonic orbits of period-2 merges into the codimension-two bifurcation point and then disappears. In this moment, chaotic motions result from a Hopf bifurcation of a stable quasi-periodic orbit and another saddle-node bifurcation. A Manneville-Pomeau and a Ruelle-Takens-Newhouse routes to the chaotic trajectories are observed. The disappearance of the Hopf bifurcation of period-2 at the codimension-two bifurcation point induces chaos was not studied.

Some approaches are applied to analyze the dynamics of the asymmetric nonautonomous system. Periodic orbits of the system are detected by the shooting method [Kawakami, 1984]. Then the stability of the periodic orbits is performed

through Floquet theory [Friedmann & Hammond, 1977; Hsu, 1972; Nayfeh & Mook, 1979]. Based on the parametric continuation algorithm [Padmanabhan & Singh, 1995], bifurcation points and bifurcation lines constructed by the bifurcation points are obtained with varying parameters of the nonlinear system. Besides, frequency responses are calculated via the harmonic balance method [Hayashi, 1964]. The analysis results provide information about the novel dynamics of the coupled system.

2. Detection of periodic orbits and subharmonic orbits

A nonautonomous system in which a periodic excitation is involved is illustrated as,

$$\dot{\mathbf{x}} = \mathbf{F}(\mathbf{x}, \omega t), \quad (1)$$

where ω denotes the frequency of the periodic excitation. The shooting method [Kawakami, 1984] is an approach of detecting periodic orbits of period-1 and subharmonic orbits of period- k of the system via a Poincaré section that stroboscopically samples a point on a trajectory of the system per period of the orbit. The orbits correspond to fixed points on the section. In the following, the fixed points are detected through a Poincaré map that is mapping of an intersection point of a trajectory with the Poin-

caré section onto the subsequent intersection point. Selecting some values \mathbf{y}_0 as the starting point of the procedure of the detection corresponding to the time $t=0$, the Poincaré map $\mathbf{G}(\mathbf{y}_0)$ of the point \mathbf{y}_0 is obtained by numerically integrating Eq. (1) with a initial value \mathbf{y}_0 and computing the solution $\mathbf{x}(t, \mathbf{y}_0)$ at the period kT ,

$$\mathbf{G}: \mathbf{R}^n \rightarrow \mathbf{R}^n; \mathbf{y}_0 \mapsto \mathbf{G}(\mathbf{y}_0) = \mathbf{x}(kT, \mathbf{y}_0), \quad (2)$$

where T is the period of the harmonic excitation. A fixed point \mathbf{y}^* that corresponds to a periodic orbit or a subharmonic orbit $\bar{\mathbf{x}}$ of Eq. (1) on the Poincaré section can be determined through zeros of the equation given below,

$$\mathbf{G}(\mathbf{y}) - \mathbf{y} = 0. \quad (3)$$

The orbit $\bar{\mathbf{x}}$ is accounted by numerically integrating Eq. (1) with the initial value \mathbf{y}^* among one period kT .

The harmonic balance method [Hayashi, 1964] is another approach to approximate the periodic orbits and subharmonic orbits of the system. The periodic orbit of period-1 or the subharmonic orbit of period- k is approximated by truncated trigonometric functions,

$$x_l(t) = \alpha_{0l} + \sum_{i=1}^N \alpha_{il} \cos\left(\frac{t}{k} \cdot \omega + \beta_{il}\right), \quad l=1 \sim n, \quad (4)$$

where x_l is the l -th element of \mathbf{x} and α_{0l} , $\alpha_{\frac{l}{k}}$, and $\beta_{\frac{l}{k}}$ are $n \cdot (2N+1)$ unknown Fourier coefficients. The value of the positive integer N depends on the required accuracy of the approximation. Substitution of Eq. (4) into Eq. (1) and balancing the coefficients of each of the harmonic terms produce $n \cdot (2N+1)$ nonlinear algebra equations in terms of the $n \cdot (2N+1)$ unknown Fourier coefficients. Using those $n \cdot (2N+1)$ equations, the Fourier coefficients can be numerically calculated. In this study, frequency responses of the system are obtained via the harmonic balance method.

3. Stability of periodic orbits and subharmonic orbits

This study obtains the stability of periodic orbits and subharmonic orbits via Floquet theory [Friedmann & Hammond, 1977; Hsu, 1972; Nayfeh & Mook, 1979]. Small perturbation to a periodic orbit or a subharmonic orbit determines the stability of the orbit by linearizing the full equations of motion in relation to the orbit. The result of the linearization is a linear, time variant differential equation.

To perturb a orbit $\tilde{\mathbf{x}}$, this study substitutes $\mathbf{x} = \bar{\mathbf{x}} + \tilde{\mathbf{x}}$ into Eq. (1). $\tilde{\mathbf{x}}$ represents small perturbation of the orbit $\bar{\mathbf{x}}$. The orbit $\bar{\mathbf{x}}$ was evaluated through the shooting method or the harmonic balance method which is described in the previous

section. Preserving only the linear terms of the equation, the perturbed system can be described as follows,

$$\dot{\tilde{\mathbf{x}}} = A(t) \tilde{\mathbf{x}}, \quad (5)$$

where $A(t)$ is a matrix of time-periodic coefficients. The transition matrix $T_\lambda(\bar{\mathbf{x}})$, which determines the stability of the orbit $\bar{\mathbf{x}}$, is calculated numerically from the matrix $A(t)$ with a Runge-Kutta scheme [Friedmann & Hammond, 1977]. The characteristic equation of $T_\lambda(\bar{\mathbf{x}})$ is written as follows,

$$\chi(\bar{\mathbf{x}}, \lambda, \mu) = \det(\mu I - T_\lambda(\bar{\mathbf{x}})) = \mu^n + a_1 \mu^{n-1} + \dots + a_{n-1} \mu + a_n = 0, \quad (6)$$

where I is an $n \times n$ identify matrix, μ is a eigenvalue of the matrix $T_\lambda(\bar{\mathbf{x}})$, and λ is the system parameter. According to the Floquet theory, the orbit $\bar{\mathbf{x}}$ is stable if all eigenvalues of its transition matrix have modules less than unity; otherwise it is unstable. A bifurcation occurs in the eigenvalues passing through the unit circle of the complex plane; i.e., one or more the eigenvalues of the transition matrix have unity modulus,

$$\mu = \cos\theta + j \sin\theta, \quad 0 \leq \theta \leq 2\pi, \quad (7)$$

where $j = \sqrt{-1}$. Three types of instabilities are shown as follows: (i) $\theta = \pi$, period dou-

bling bifurcation occurs; (ii) $\theta=0$, saddle-node bifurcation, pitchfork bifurcation or transcritical bifurcation occurs; (iii) $\theta \neq 0$ and $\theta \neq \pi$, Hopf bifurcation occurs. Substituting Eq. (7) into Eq. (6), bifurcation points are obtained by the detection methods and the parametric continuation algorithm [Padmanabhan & Singh, 1995].

4. Codimension-two bifurcation in a coupled Duffing equation with twisted frequency-response curves

Consider a coupled asymmetric nonautonomous system that is illustrated as follows [Hsiao & Tung, 1999]:

$$\begin{aligned} \ddot{x}_1 + \lambda_c \dot{x}_1 + [k_{c1}x_1 + k_{c3}(x_1^3 - 3\delta_{x1} \cdot x_1^2 + 3\delta_{x1}^2 \cdot x_1)] - \mu \cdot \lambda_a (\dot{x}_2 - \dot{x}_1) - \\ \mu \{k_{a1}(x_2 - x_1) + k_{a3}[(x_2 - x_1)^3 + 3(\delta_{x1} - \delta_{x2})^2(x_2 - x_1) + \\ 3(\delta_{x1} - \delta_{x2})(x_2 - x_1)^2]\} = m_e r \omega^2 \cos(\omega \cdot t), \end{aligned} \quad (8a)$$

$$\begin{aligned} \ddot{x}_2 + \lambda_a (\dot{x}_2 - \dot{x}_1) + \{k_{a1}(x_2 - x_1) + k_{a3}[(x_2 - x_1)^3 - \\ 3(\delta_{x2} - \delta_{x1})(x_2 - x_1)^2 + 3(\delta_{x2} - \delta_{x1})^2(x_2 - x_1)]\} = 0. \end{aligned} \quad (8b)$$

Table 1 shows the parameters of Eqs. (8a) and (8b). The equations of the coupled system are derived from a nonlinear dynamic absorber. In the following, periodic orbits and subharmonic orbits for the equations are detected by using the shooting method and frequency responses of the system are obtained through the harmonic balance method as described in Section II. Besides, the stability of the obtained orbits is performed using the Floquet theory as illustrated in Section III. For the stability analysis, the bifurcation points can be ob-

tained and the bifurcation lines are constructed as the parameters are changed.

Fig. 1(a) portrays a two-parametric bifurcation diagram on a parameter plane (ω, r) . Bifurcation lines $L_{sn1,a}, L_{sn1,b}, L_{sn1,c}, L_{sn1,d}, L_{sn2,a}, L_{sn2,b}, L_{sn2,c}, L_{sn2,d}, L_{sn2,e}, L_{sn2,f}, L_{sn2,g}, L_{pd1,a}, L_{pd1,b}, L_{pd1,c}, L_{pd1,d}, L_{pd1,e}, L_{pd1,f}, L_{pd2,a}, L_{pd2,b}, L_{pd2,c}, L_{pd2,d}, L_{H2,a}, L_{H2,b}, L_{H2,c}, L_{H2,d},$ and $L_{H2,e}$ as shown in Fig. 1(a) are constructed by the saddle-node bifurcation points $P_{sn1,a}, P_{sn1,b}, P_{sn1,c}, P_{sn1,d}, P_{sn2,a}, P_{sn2,b}, P_{sn2,c}, P_{sn2,d}, P_{sn2,e}, P_{sn2,f}, P_{sn2,g},$ the period doubling bifurcation points $P_{pd1,a}, P_{pd1,b},$

Novel Codimension-two Bifurcation in a Coupled Duffing System with twisted
frequency-response curves / Yung-Chia Hsiao · Ting-Yu Lai

$P_{pd1,c}$, $P_{pd1,d}$, $P_{pd1,e}$, $P_{pd1,f}$, $P_{pd2,a}$, $P_{pd2,b}$, $P_{pd2,c}$, $P_{pd2,d}$, and the Hopf bifurcation points $P_{H2,a}$, $P_{H2,b}$, $P_{H2,c}$, $P_{H2,d}$, $P_{H2,e}$. Fig. 1(b) is a blow-up of Fig. 1(a) around the point P_a . The period doubling bifurcation line $L_{pd1,b}$ tangentially intersects the saddle-node bifurcation line $L_{sn1,b}$ at a codimension-two bifurcation point P_a . The Hopf bifurcation line $L_{H2,d}$ intersects the point P_a and then disappears in the point. Furthermore, Fig. 2 schematically portrays the bifurcation set around the codimension-two bifurcation point P_a , including fixed points of period-1, sub-harmonic orbit of period-2, almost periodic orbits, and chaos on the bifurcation lines $L_{sn1,b}$ and $L_{sn1,d}$ and in Regions I to X. The details about Fig. 2 will be described in the last paragraphs of this section. To describe transparently the previous phenomenon, frequency responses along two dashdot lines L_1 and L_2 of Fig. 1(b) at $r=0.263$ and $r=0.27$ respectively, are illustrated in the following.

Fig. 3 shows the frequency response of the system at $r=0.263$. α_{11} and $\alpha_{\frac{1}{2}1}$ are the frequency-response curve of periodic orbits of period-1 and subharmonic orbits of period-2, respectively. Fig. 3 also portrays that the frequency-response curve α_{11} is twisted to the left and then to the right. The points $P_{sn1,a}$, $P_{sn1,b}$, and $P_{sn1,d}$ are the saddle-node bifurcation points of the periodic orbits. The points $P_{pd1,a}$, $P_{pd1,b}$, $P_{pd1,c}$, $P_{pd1,d}$, $P_{pd1,e}$, and $P_{pd1,f}$ are the period dou-

bling bifurcation points of the periodic orbits. The subcritical period doubling bifurcation point $P_{pd1,a}$ and the supercritical period doubling bifurcation point $P_{pd1,b}$ are at the left side of the saddle-node bifurcation point $P_{sn1,b}$. Subharmonic orbits of period-2 bifurcate from the period doubling bifurcation points $P_{pd1,a}$ and $P_{pd1,b}$. Furthermore, there are some bifurcations in the subharmonic orbits, such as the saddle-node bifurcation points $P_{sn2,a}$, $P_{sn2,b}$, $P_{sn2,c}$, $P_{sn2,d}$, and $P_{sn2,e}$ and the periodic bifurcation points $P_{pd2,a}$, $P_{pd2,b}$, $P_{pd2,c}$, and $P_{pd2,d}$. Besides, the stable subharmonic orbits loss their stability at Hopf bifurcation points $P_{H2,a}$, $P_{H2,b}$, $P_{H2,c}$, and $P_{H2,d}$. To classify the bifurcation points of the periodic orbits of period-1 and the points of the subharmonic orbits of period-2, the symbol ‘○’ denotes the bifurcation points of the periodic orbits of the period-1 and the symbol ‘●’ represents the bifurcation points of the subharmonic orbits of period-2.

With increasing the values of the parameter r , The Hopf bifurcation points $P_{H2,c}$ and $P_{H2,d}$ runs away each other, and the period doubling bifurcation point $P_{pd1,b}$ is close to the saddle-node bifurcation point $P_{sn1,b}$. Then the point $P_{pd1,b}$ crosses the saddle-node bifurcation point $P_{sn1,b}$ and then moves to the unstable branch. Meanwhile, the Hopf bifurcation point $P_{H2,d}$ coalesces into the period doubling bifurcation point $P_{pd1,b}$ in the same time. This cross results in the

codimension-two bifurcation described in Fig. 1(b). Fig. 4 illustrates the frequency response at $r=0.27$ after this cross. The Hopf bifurcation point $P_{H2,d}$ have been disappeared and the period doubling bifurcation point $P_{pd1,b}$ locates at the upper of the saddle-node bifurcation point $P_{sn1,b}$.

The disappearance of the bifurcation point $P_{H2,d}$ results in chaos. Fig. 5(a) describes a bifurcation diagram and Fig. 5(b) portrays Lyapunov exponents of the system for $r=0.267$. According to the investigation of Wolf et al. [Wolf et al., 1985], a motion with one or more positive Lyapunov exponents is defined to be chaotic. Fig. 5(b) confirms that chaotic motions locate in an interval between $\omega \approx 0.97$ and $\omega \approx 1.04$. A Ruelle-Takens-Newhouse route to chaos [Schuster, 1984] occurs at $\omega \approx 0.97$. A stable quasi-periodic orbit is translated to a chaotic trajectory through a Hopf bifurcation. Fig. 6 illustrates a chaotic attractor on the Poincaré section for $\omega = 1.03$. In addition, the chaotic motions vanish for $\omega > 1.04$ due to the existence of stable periodic orbits that result from a saddle-node bifurcation point $P_{sn1,d}$. The phenomenon is called the Manneville-Pomeau route to chaos.

By the aid of Figs. 3 to 6, the bifurcation set around the codimension-two bifurcation point P_a can be clearly and completely described as follows. Fig. 2 schematically shows the bifurcation set around the codimension-two bifurcation point P_a . The point P_1 denotes the fixed point at the

left of the saddle-node bifurcation point $P_{sn1,b}$. The points P_2, P_3 , and P_4 display the fixed points between the bifurcation points $P_{sn1,a}$ and $P_{sn1,b}$, $P_{sn1,a}$ and $P_{sn1,c}$, $P_{sn1,c}$ and $P_{sn1,d}$, respectively. The point P_5 is the fixed point at the right of the bifurcation point $P_{sn1,d}$. In this figure, the period doubling bifurcation line $L_{pd1,b}$ tangentially interests the saddle-node bifurcation line $L_{sn1,b}$ at the point P_a . Meanwhile, the Hopf bifurcation lines $L_{H2,d}$ and $L_{pd1,b}^1$ interest the point P_a and then disappear. The bifurcation line $L_{sn1,d}$ is the saddle-node bifurcation that does not interest the others. The bifurcation lines divide the parameter plane (ω, r) around the codimension-two bifurcation point P_a into ten regions that are denoted as Regions I, II, III, IV, V, VI, VII, VIII, IX, and X, respectively. Make a roundtrip near the codimension-two bifurcation point P_a , starting from Region I where there are three fixed points. The upper and lower fixed points P_3 and P_5 are stable and the middle fixed point P_4 is unstable. Entering from Region I into Region II through the lower component $L_{sn1,b}^1$ of the saddle-node bifurcation line $L_{sn1,b}$ yields two fixed points: a stable fixed point P_1 and an unstable fixed point P_2 . Then the stable fixed point P_1 loses its stability and simultaneously a stable subharmonic orbit of period-2 is generated in crossing the supercritical component $L_{pd1,b}^1$ of the period doubling bifurcation line $L_{pd1,b}$. The same variation is occurs in crossing the period doubling bifurcation line

$L_{pd1,b}^1$ from Region X into Region IV. If one continues the journey clockwise and reaches Region IV, the stable fixed point P_5 and the unstable fixed point P_4 are coalesced each other at the saddle-node bifurcation line $L_{sn1,d}$. Entering from Region IV into Region V through the Hopf bifurcation line $L_{H2,d}$ changes the stable subharmonic orbit of period-2 to be unstable and an almost periodic orbit is generated in the same time. Continuing the journey clockwise and reaching Region VI, a stable manifold of the middle fixed point P_2 loses its stability in crossing the subcritical component $L_{pd1,b}^2$ of the period doubling bifurcation line $L_{pd1,b}$ and the unstable subharmonic orbit of period-2 simultaneously disappeared. Entering from Region VI into Region VII, two unstable fixed points P_1 and P_2 are coalesced each other at the upper component $L_{sn1,b}^2$ of the saddle-node bifurcation line $L_{sn1,b}$. In crossing the Hopf bifurcation line L_{HT} , the stable almost periodic orbit loses its stability and then simultaneously generates a chaotic orbit when entering from Region VII into Region VIII. Meanwhile, the chaotic orbit is disappeared when the Hopf bifurcation line $L_{H2,d}$ is generated from the codimension-two bifurcation point P_a in Region IX. Finally, returning to Region I through the saddle-node bifurcation line $L_{sn1,d}$ yields two fixed points: a stable fixed point P_5 and an unstable fixed point P_4 . According to the bifurcation theory [Kuznetsov, 1995], the codimension-two bifurcation set is com-

pletely. The supercritical period doubling bifurcation is changed to be subcritical when the period doubling bifurcation line $L_{pd1,b}$ passes through the codimension-two bifurcation point P_a . Meanwhile, the saddle-node bifurcation with the coalescence of a stable periodic orbit and an unstable periodic orbit is changed to the bifurcation with the coalescence with two unstable periodic orbits. Besides, the Hopf bifurcation lines $L_{H2,d}$ and L_{HT} are generated from the codimension-two point. Chaos is extremely important in the codimension-two bifurcation.

5. Conclusions

This paper studied a novel codimension-two bifurcation combined by chaos and the bifurcations of the periodic orbits of period-1 and the subharmonic orbits of period-2 was observed in the coupled Duffing system with twisted frequency-response curves. The bifurcation line constructed by the saddle-node bifurcations of the periodic orbits of period-1 tangentially intersects the bifurcation line constructed by the period doubling bifurcations of the periodic orbits of period-1 at the codimension-two bifurcation point. Besides, the Hopf bifurcation line merges into the point and then disappears. In this moment, the chaotic motions result from the Hopf bifurcation of the stable quasi-periodic orbit. A Manneville-Pomeau and a Ruelle-Takens-Newhouse routes to the chaotic

trajectories are observed. The disappearance of the Hopf bifurcation of subharmonic orbits of period-2 at the codimension-two bifurcation point induces chaos was not studied in another investigation.

Some approaches were applied to analyze the dynamics of the asymmetric nonautonomous system. The periodic orbits of the system are detected by the shooting method. Then the stability of the periodic orbits is performed through Floquet theory. Based on the parametric continuation algorithm, bifurcation points and bifurcation lines constructed by the bifurcation points are obtained with varying parameters of the nonlinear system. Besides, frequency responses are calculated via the harmonic balance method. The analysis results provide information about the novel dynamics of the coupled system.

References

- Friedmann, P. and Hammond, C. E. (1977) Efficient numerical treatment of periodic systems with application to stability problems, *International Journal for Numerical Methods in Engineering*, Vol. 11, pp. 1117-1136.
- Hayashi, C. (1964) *Nonlinear oscillations in physical systems*, Princeton University Press, Princeton, pp. 28-30.
- Hsiao, Yung-Chia and Tung, Pi-Cheng (1999) Nonlinear dynamics of the asymmetric vibration absorber, *Proceedings of the 16th National Conference of the Chinese Society of Mechanical Engineers*, pp. 911-919.
- Hsiao, Yung-Chia and Tung, Pi-Cheng (2002) Mechanism of Producing a Saddle-Node Bifurcation with the Coalescence of Two Unstable Periodic Orbits, *Chaos, Solitons and Fractals*, Vol.13, pp. 1429-1438.
- Hsu, C. S. (1972) Impulsive parametric excitation: theory. *Journal of Applied Mechanics, Transactions of the ASME*, Vol. 39, pp. 551-558.
- Kawakami, H. (1984) Bifurcation of periodic responses in forced dynamic nonlinear circuits: computation of bifurcation values of the system parameters. *IEEE Transactions on Circuits and Systems*, Vol. CAS-31, pp. 248-260.
- Kuznetsov, Y. A. (1995) *Elements of Applied Bifurcation Theory*, New York, Springer,-Verlag.
- Nayfeh, A. H. and Mook, D. T. (1979) *Nonlinear oscillations*, New York, John Wiley & Sons, pp. 273-283.
- Padmanabhan, C. and Singh, R. (1995) Analysis of periodically excited non-linear systems by a parametric continuation technique, *Journal of Sound Vibration*, Vol. 184, pp. 35-58.
- Schuster, H. G. (1984) *Deterministic Chaos — an Introduction*, Physik-Verlag, Weinheim, pp. 126-130.
- Szemplińska-stupnicka, Wanda (1990) *The Behavior of Nonlinear Vibrating Sys-*

Novel Codimension-two Bifurcation in a Coupled Duffing System with twisted frequency-response curves / Yung-Chia Hsiao · Ting-Yu Lai

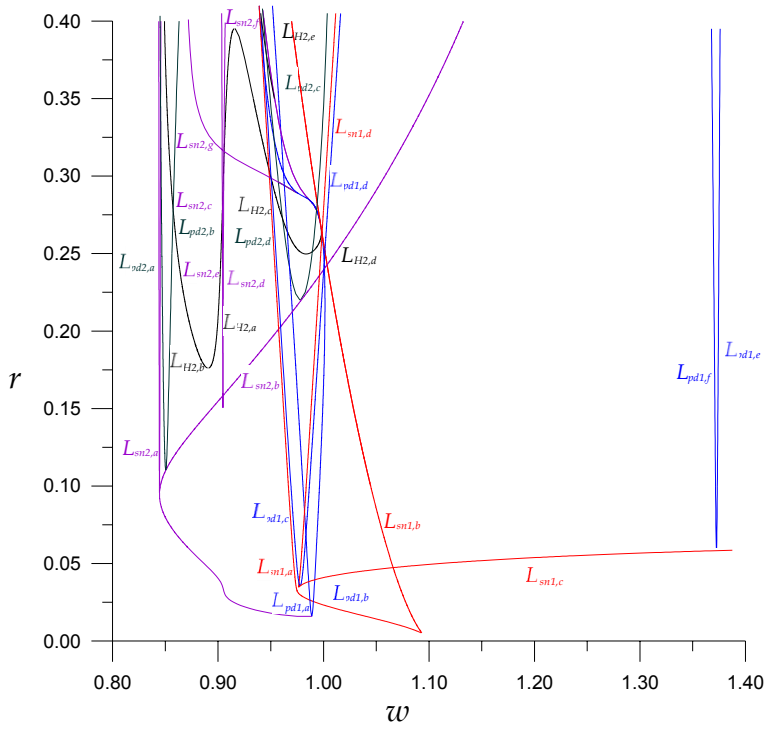
tem, Volume I, Dordrecht, Kluwer Academic Publishers, pp. 136.

Vastano, J. A. (1985) Determining Lyapunov Exponents from a Time Series, Physica 16D, pp. 285-317.

Wolf, A., Swift, J. B., Swinney, H. L., and

Table 1 System parameters of Eqs. (8a) and (8b).

Parameters	Values
η	0.769
λ_c	0.03209
k_{c1}	0.0708
k_{c3}	40.31473
δ_{x1}	0.06917
λ_a	0.0025
k_{a1}	0.09208
k_{a3}	52.43516
δ_{x2}	0.11726
m_e	0.00992



(a)

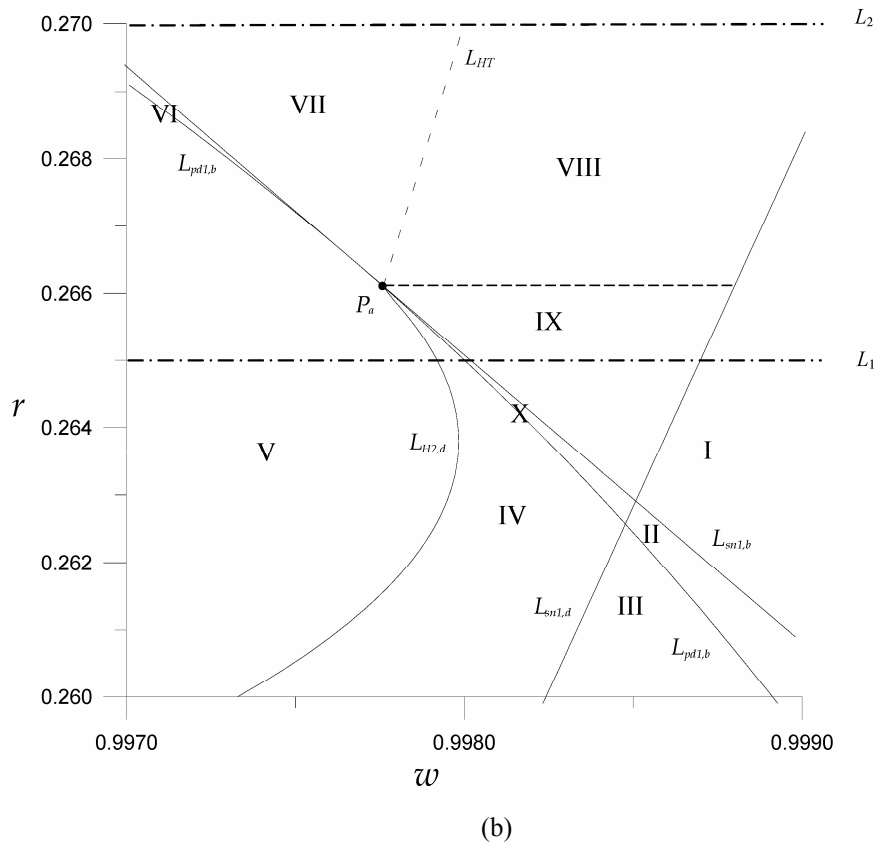


Fig. 1 (a) Bifurcation set for the codimension-two bifurcation. (b) A blow-up of Fig.1(a) around the codimension-two bifurcation point P_a .

Novel Codimension-two Bifurcation in a Coupled Duffing System with twisted frequency-response curves / Yung-Chia Hsiao, Ting-Yu Lai

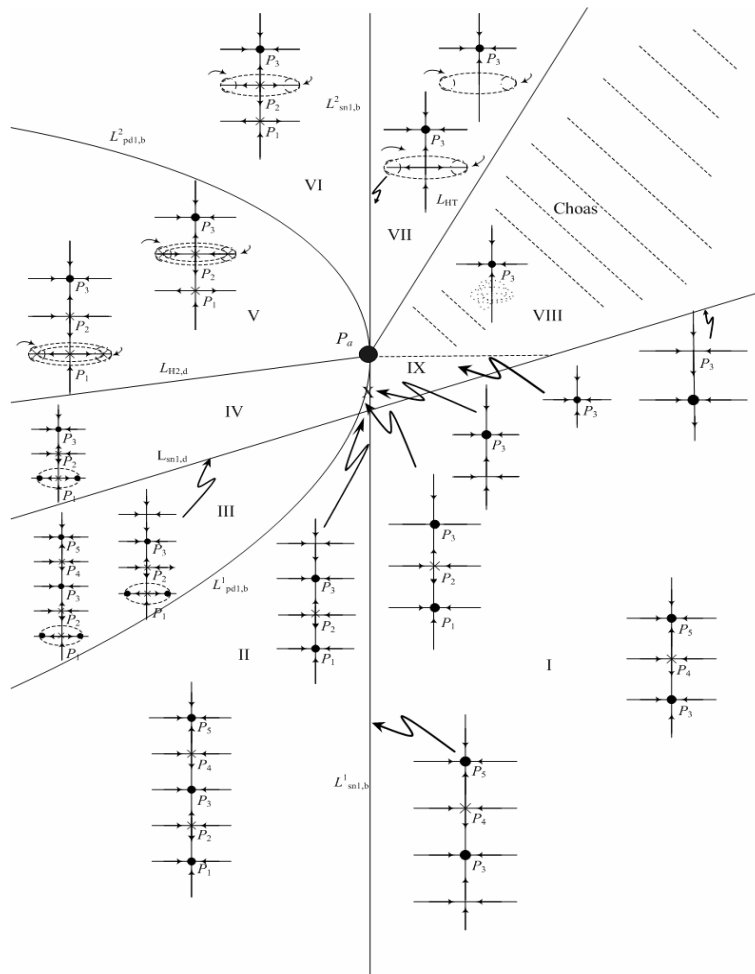


Fig. 2 A schematic diagram of the bifurcation set.

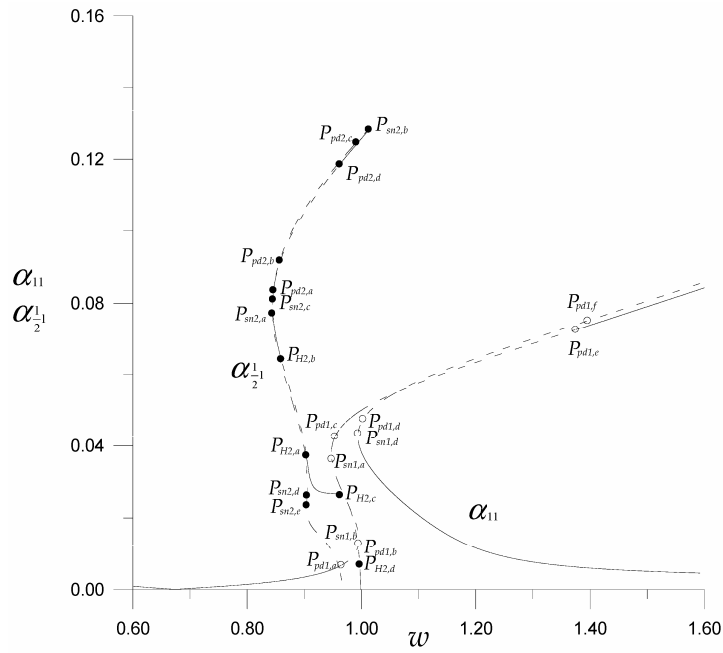


Fig. 3 Frequency response of the system at $r=0.263$.

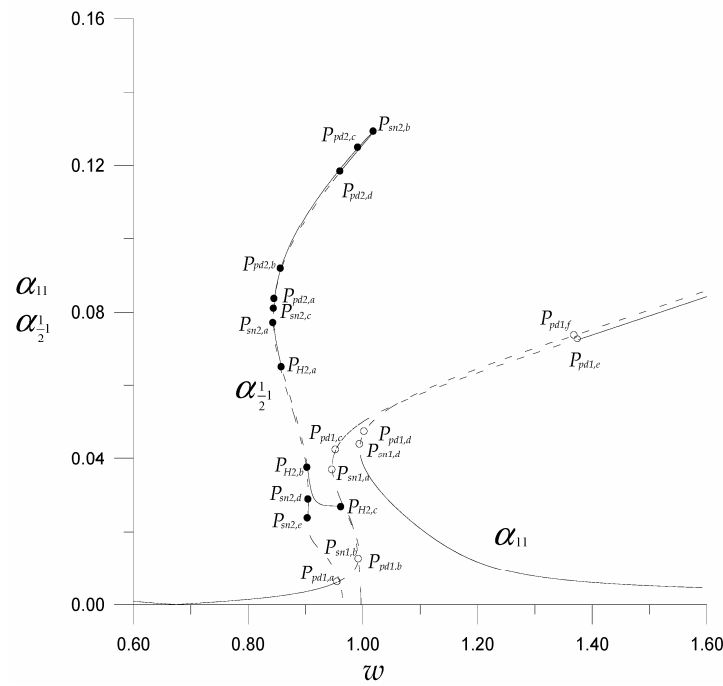
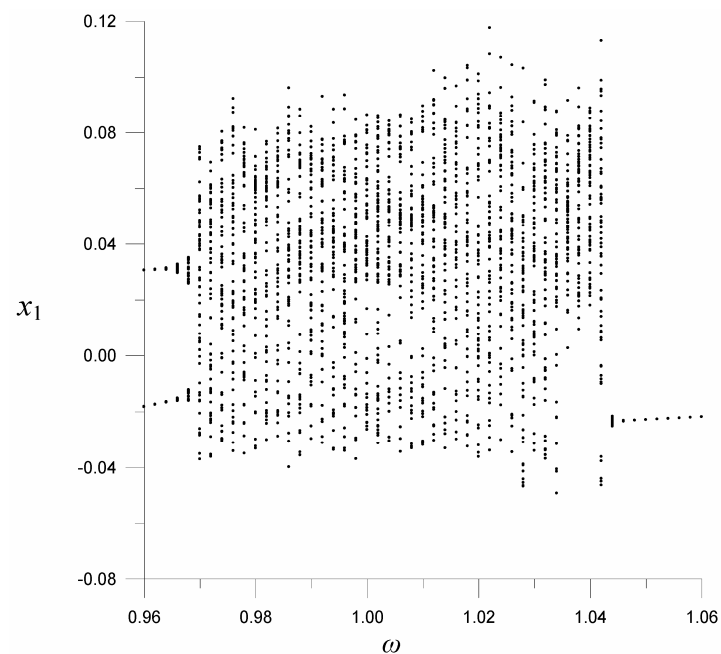
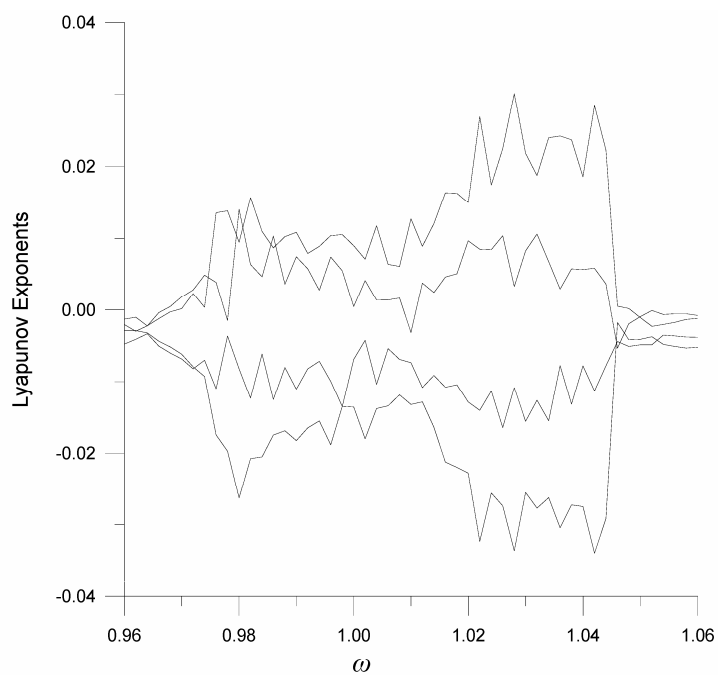


Fig. 4 Frequency response of the system at $r=0.27$.

Novel Codimension-two Bifurcation in a Coupled Duffing System with twisted frequency-response curves / Yung-Chia Hsiao, Ting-Yu Lai



(a)



(b)

Fig. 5 (a) Bifurcation diagram of the system for $r=0.267$. (b) Lyapunov exponents of the system.

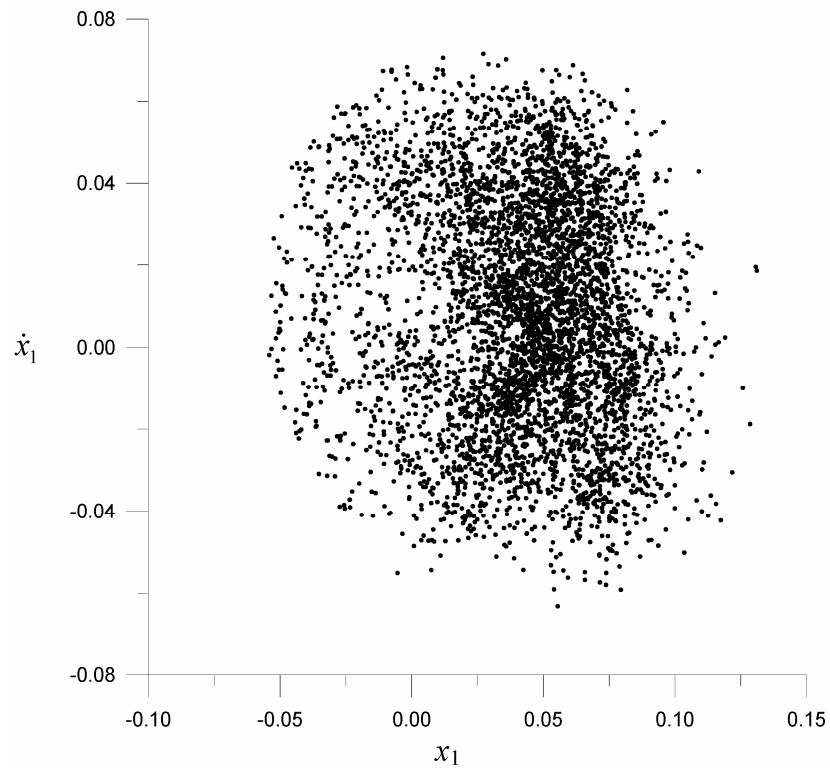


Fig. 6 Chaotic attractor on the Poincaré section for $r=0.267$ and $\omega=1.03$.

具彎曲頻率響應曲線耦合杜飛系統之新 共維度二分歧現象

蕭永嘉^{1*} 賴廷裕²

¹ 明道大學資訊工程學系助理教授

² 國立中央大學機械工程研究所博士班研究生

摘 要

本論文發現在某些參數下具彎曲頻率響應曲線之耦合杜飛系統在某些參數下產生新共維度二分歧現象。此現象由週期加倍分歧、鞍點-節點分歧、霍伯夫分歧及混沌運動所組成。週期運動之鞍點-節點分歧線與週期加倍分歧線相交於一共維度二分歧點，而次簡協運動之霍伯夫分歧線與此點相交後消失並同時產生混沌運動。為分析上述現象，文中應用發射法求得系統之週期解及次簡諧解，而頻譜響應圖則以簡諧平衡法求之。其穩定性分析則利用 Floquet 理論求得。

關鍵字：分歧，共維度二，混沌，杜飛系統，次簡諧運動